Multiport Analysis of Hexagonal Patch Antenna

Sajid Muhaimin Choudhury, Md. Abdul Matin
Department of EEE, Bangladesh University of Engineering and Technology
Email (smc@ieee.org)

Abstract: This paper demonstrates application of multiport analysis technique to a hexagonal patch antenna. The multiport analysis technique is applied to construct a lumped element circuit model of a hexagonal patch antenna. FEM simulation of the hexagonal patch is also performed and the effect of varying patch dimension is observed. The results show that a basic hexagonal patch structure results in patch size reduction compared to rectangular patch for the same center frequency.

Keywords – patch antenna; multiport analysis

I. INTRODUCTION

Microstrip Patch Antennas (MSA) are widely used for their low profile characteristics. They are electrically thin, light weight, easy to fab- ricate and low cost antennas. Various methods of analysis for MSA has been developed, including Transmission line model [1, 2], Cavity model [3, 4] and Finite Element method [5]. For arbitrary shaped patch structure Finite Element Method is suitable. Gupta introduced the technique of Multi-port Analysis [2] for solving arbitrary shaped patch structure. The patch itself is modelled by interconnection of basic shaped patches. The radiation is modelled by loading ports of outer periphery. The method has multiple applications, such as Pad´e approximation [6] can be used to predict resonant behaviour of antenna from input impedance

Hexagonal structures have space filling properties. They are used in array antenna applications to reduce return loss and mutual coupling [7]. Dubey et al. proposed dual frequency broadband hexagonal microstrip antenna and observed to have 10.2% bandwidth improvement [8]. In this paper, Multiport Network analysis technique is applied to a Hexagonal Patch antenna structure. Also, the radiation characteristics of the antenna is studied using Finite Element Method.

II. MULTIPORT NETWORK ANALYSIS

A. *Segmentation Method*

Figure 1 shows the structure of a basic hexagonal patch antenna. For the analysis performed, it is assumed that the patch has a thin substrate. For simulation, FR-4 substrate is used.

For a shape for which the Green's function is defined as the doubly infinite summation with terms corresponding to various modes of planar resonance with magnetic wall, the Z matrix characterization can be written as [2],

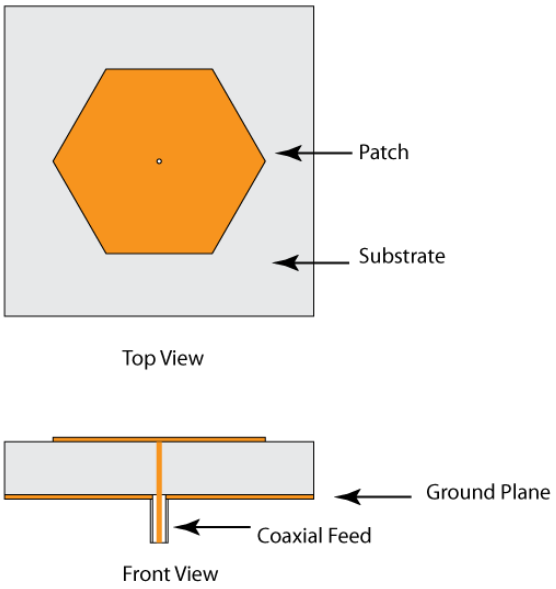

Figure 1. Basic Hexagonal Patch structure

$$Z_{ij} = \frac{1}{W_i W_j} \int_{W_i} \int_{W_j} G(x_i, y_i \mid x_j, y_j) ds_i ds_j \qquad (1)$$

where, *Zij* is Z parameter between port ith and jth

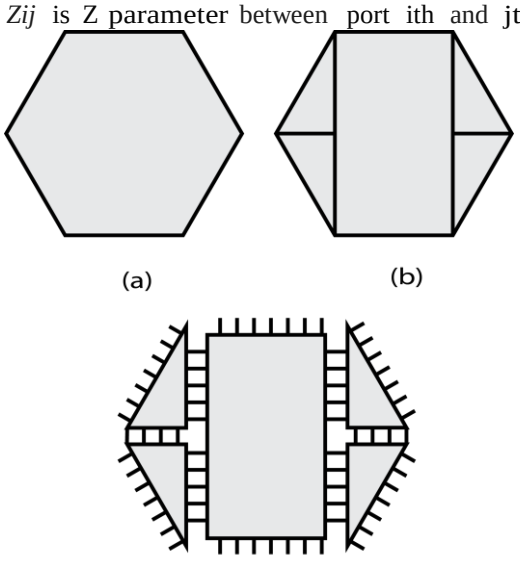

Figure 2. (a) Basic Hexagonal Structure (b) Structure divided into triangles and rectangle (c) Multiport Representation of a hexagonal patch

B. *Z-matrix for basic rectangular and triangular segments*

The Green's function for rectangular patch is given by [9],

$$G(x_i, y_i \mid x_j, y_j) = \frac{j\omega\mu d}{ab}\sum_{n=0}^{\infty}\sum_{m=0}^{\infty}\left[\frac{\sigma_m\sigma_n cos(k_y y_0)cos(k_x x_0)}{k_x^2 + k_y^2 - k^2} \times cos(k_x x)cos(k_y y)\right] \quad (2)$$

Where,

$$k_x = \frac{m\pi}{a}$$

$$k_y = \frac{n\pi}{b}$$

$$k^2 = \omega^2\mu\grave{o}_0\grave{o}_r(1 - j\delta) \quad (3)$$

$$\sigma_i = \begin{cases} 1, i = 0 \\ 2, i \neq 0 \end{cases}$$

Here, μ is Magnetic Permeability of Dielectric Medium, ϵ is Electric Permittivity of Medium, ω is Angular Frequency, δ is Loss Tangent.

Green's function for right angled $30^\circ - 60^\circ$ triangle can be written as [10],

$$G(x_i, y_i \mid x_j, y_j) = 8j\omega\mu d\sum_{n=0}^{\infty}\sum_{m=0}^{\infty}\frac{T_l(x_0, y_0)T_l(x, y)}{\left(16\sqrt{3}\pi^2(m^2 + mn + n^2) - 9\sqrt{3}a^2k^2\right)} \quad (4)$$

Where,

$$T_l(x, y) = (-1)^l cos\left(\frac{2\pi lx}{\sqrt{3}a}\right)cos\left[\frac{2\pi(m-n)y}{3a}\right] + (-1)^m cos\left(\frac{2\pi mx}{\sqrt{3}a}\right)cos\left[\frac{2\pi(n-l)y}{3a}\right] + (-1)^n cos\left(\frac{2\pi nx}{\sqrt{3}a}\right)cos\left[\frac{2\pi(l-m)y}{3a}\right] \quad (5)$$

By substituting value of Green's function into Equation 1 the Z- matrix components can be computed. For rectangular patch, for two ports p and q located at (x_p, y_p) and (x_q, y_q) the components of Z- matrix can be obtained by the equation suggested by Benalla et al. [11],

$$Z_{pq} = \frac{j\omega\mu d}{ab}\sum_{m=0}^{\infty}\sum_{n=0}^{\infty}\frac{\sigma_m\sigma_n\phi_{mn}(x_p, y_p)\phi_{mn}(x_q, y_q)}{k_x^2 + k_y^2 - k^2} \quad (6)$$

For ports oriented along y direction, the value of $\phi_{mn}(x, y)$ is given by

$$\phi_{mn}(x, y) = cos(k_x x)cos(k_y y)sinc\left(\frac{k_y w}{2}\right) \quad (7)$$

and for ports oriented along x direction

$$\phi_{mn}(x, y) = cos(k_x x)cos(k_y y)sinc\left(\frac{k_y w}{2}\right) \quad (8)$$

Faster computation of above parameters are possible by reducing the double integral to single integral [11]. If port p and q are oriented along the same direction, the Z parameter for port p and q can be obtained by,

$$Z_{pq} = -CF\frac{1}{\eta}\left[\sum_{l=0}^{L}\left(\frac{\sigma_l cos(k_u u_p)cos(k_u u_q)}{\gamma_l sin(\gamma_l F)} \times cos(\gamma_l z_>)cos(\gamma_l z_<) \times sinc\left(\frac{k_u w_p}{2}\right)sinc\left(\frac{k_u w_p}{2}\right)\right)\right] - jCF\frac{1}{\eta}\left[\sum_{l=L+1}^{\infty}\left(\frac{cos(k_u u_p)cos(k_u u_q)sinc\left(\frac{k_u w_p}{2}\right)}{\gamma_l} \times sinc\left(\frac{k_u w_p}{2}\right)e^{-j\gamma_l(v_> - v_<)}\right)\right] \quad (9)$$

where, condition is set that if both ports p and q are oriented along y direction, $l = m$ condition is set, and if both ports are located along x direction, $l = n$ is chosen.

For ports p and q oriented along different direction, (x and y) the Z parameter matrix elements can be obtained by,

$$Z_{pq} = -CF\frac{1}{\eta}\left[\sum_{l=0}^{L}\left(\frac{\sigma_l cos(k_u u_p)cos(k_u u_q)}{\gamma_l sin(\gamma_l F)} \times cos(\gamma_l z_>)cos(\gamma_l z_<) \times sinc\left(\frac{k_u w_p}{2}\right)sinc\left(\frac{\gamma_l w_q}{2}\right)\right)\right] - jCF\frac{1}{\eta}\left[\sum_{l=L+1}^{\infty}\left(\frac{cos(k_u u_p)cos(k_u u_q)}{\gamma_l^2 w_q} \times sinc\left(\frac{k_u w_p}{2}\right) \times e^{-j\gamma_l(v_> - v_< - w_q/2)}\right)\right] \quad (10)$$

The summation bound l is chosen so that the summation is converged, and thus

$$l = m, \text{if } y_> - y_< - w_{j/2} > 0$$
$$l = n, \text{if } x_> - x_< - w_{j/2} > 0 \quad (11)$$

and if both the condition are satisfied, any choice of $l = m$ or $l = n$ would result in convergence.
The different parameter values can be obtained by,

$$F = \begin{cases} b, \text{if } l = m \\ a, \text{if } l = n \end{cases}$$

$$(u_p, u_q) = \begin{cases} (x_p, x_q), \text{if } l = m \\ (y_p, y_q), \text{if } l = n \end{cases}$$

$$\gamma_l = \pm\sqrt{k^2 - k_u^2}$$

$$k_u = \begin{cases} \dfrac{m\pi}{a}, \text{if } l = m \\ \dfrac{n\pi}{b}, \text{if } l = n \end{cases}$$

$$(z_>, z_<) = \begin{cases} (y_> - b, y_<), \text{if } l = m \\ (x_> - a, x_<), \text{if } l = n \end{cases}$$

According to Lee [12], right angled 30° – 60° triangle the Z matrix can be computed as,

$$Z_{pq} = 8j\omega\mu h \sum_{m=-\infty}^{\infty}\sum_{n=-\infty}^{\infty} \frac{I_{T_l}(p) I_{T_l}(q)}{16\sqrt{3}\pi^2(m^2+mn+n^2) - 9\sqrt{3}a^2k^2} \quad (12)$$

where $l + m + n = 1$ and a is the length of hypotenuse of the triagle, and I_{Tl} takes different values depending on the location of port p along the sides of the triangle.

- When port p is located along the side opposite to the 30° side,

$$I_{T_l}(p) = H^1(l, x_p, w_p) + H^1(m, x_p, w_p) + H^1(n, x_p, w_p) \quad (13)$$

- When port p is located along the side opposite to the 60° side,

$$I_{T_l}(p) = H^2(m-n, y_p, w_p) + H^2(n-l, y_p, w_p) + H^2(l-m, y_p, w_p) \quad (14)$$

- When port p is located along the side opposite to the 90° side,

$$I_{T_l}(p) = H^2(2(m-n), y_p, w_p/2) + H^2(2(n-l), y_p, w_p/2) + H^2(2(l-m), y_p, w_p/2) \quad (15)$$

Where functions H^1 and H^2 is given by,

$$H^1(k,t,w) = (-1)^k \cos\left(\frac{2\pi k}{\sqrt{3}a}t\right) \times sinc\left(\frac{2\pi k}{\sqrt{3}a}\frac{w}{2}\right) \quad (16)$$

$$H^2(k,t,w) = (-1)^k \cos\left(\frac{2\pi k}{3a}t\right) \quad (17)$$

The above equations were employed to calculate individual Z parameter matrix for a basic rectangular segment and 30-60-90 triangle.

C. *Segment joining to form Z-Parameter matrix of an unloaded hexagonal patch*

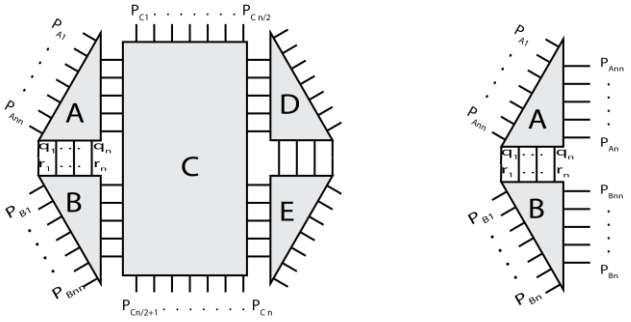

Figure 3. (a) Segmentation of unloaded hexagonal patch into part A, B, C, D, E(b) Joining part A and B

The Figure 3 a shows the segmentation of hexagon into part A, B, C, D, E where A, B, D, E are identical 30°-60° -90° triangles, for which Z parameter matrix can be calculated using Equation (12). Considering only part A and B, the two parts have some ports which are joined together, and some other ports that are unconnected and connected to other segments. For simplicity, firstly only segment A and B is considered to be joined. Segment A has external ports $\mathbf{P_A}$ and ports that are connected to B segment denoted by $\mathbf{q}$. Similarly, segment B also has $\mathbf{P_B}$ ports and ports connected to A denoted by $\mathbf{r}$. The Z matrix of each of the segments A and B can be written in terms of sub matrices as

$$\mathbf{Z_A} = \begin{bmatrix} \mathbf{Z_{p_a}} & \mathbf{Z_{p_aq}} \\ \mathbf{Z_{qp_a}} & \mathbf{Z_{qq}} \end{bmatrix}, \mathbf{Z_B} = \begin{bmatrix} \mathbf{Z_{p_b}} & \mathbf{Z_{p_br}} \\ \mathbf{Z_{rp_b}} & \mathbf{Z_{rr}} \end{bmatrix} \quad (18)$$

Combining these two arrays give,

$$\mathbf{Z_{AB}} = \begin{bmatrix} \mathbf{Z_{p_a}} & 0 \\ 0 & \mathbf{Z_{p_b}} \end{bmatrix} + \begin{bmatrix} \mathbf{Z_{p_aq}} \\ -\mathbf{Z_{p_br}} \end{bmatrix} \left[\mathbf{Z_{qq}} + \mathbf{Z_{rr}}\right] \left[-\mathbf{Z_{qp_a}} \quad \mathbf{Z_{rp_b}}\right] \quad (19)$$

The combined AB segment is identical if the segment DE is joined, and thus $\mathbf{Z_{AB}} = \mathbf{Z_{DE}}$. The port sequence of DE segment is arranged appropriately as it is attached to the opposite side of the Basic Rectangular Patch. Equation (19) can be used to compute the parameters of the pentagonal shape formed by joining segment AB and C showed in Figure 3.

D. Modeling Radiation of Hexagonal Patch

The patch shown in Figure 3 is unloaded. To find out the radiation characteristics of the patch, it has to be loaded. Figure 4 shows a Edge Admittance Network (EAN) for a typical radiating edge of a patch antenna. [13] The edge admittance network conductance corresponds to the loading, occurs due to the radiation from the patch antenna, and the capacitance corresponds to the fringing electric field .

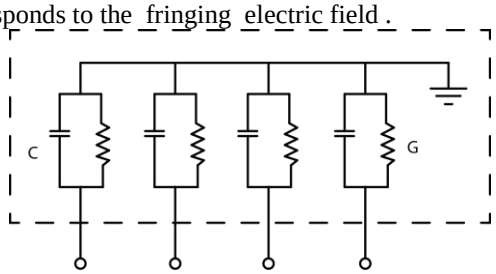

Figure 4. Edge Admittance Network

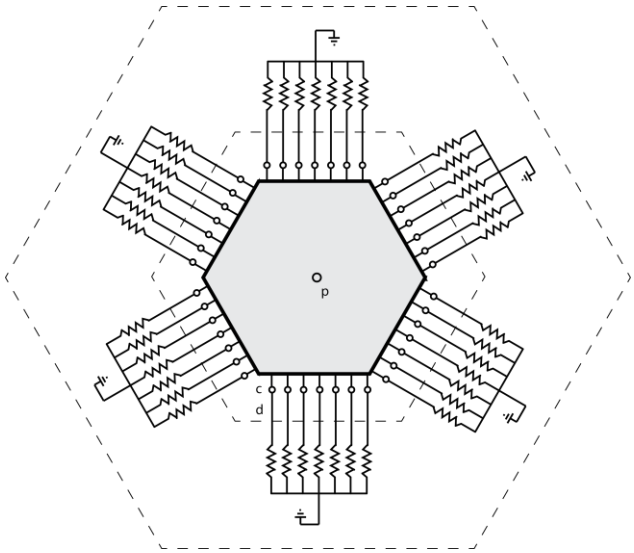

Figure 5. Loaded Hexagonal Patch Multiport Model

Loading the network shown in Figure 3 with the edge admittance network shown in Figure 4 enables to model the radiation of the patch.

The coaxial feed of the antenna is represented with equivalent planar feed. The complete multiport model of the loaded antenna is shown in Figure 5 . The entire radiation resistance network can be treated as a seperate multiport network, connected to the unloaded hexag- onal patch model. Ports corresponding to the patch and the EAN network are represented by c_i and d_i respectively. The equivalent radiation resistance can be calculated using Equation 20 for one side of the hexagonal patch element. The conductance G is then divided into all the ports parallel to one side of the hexagon.

If the width of the substrate is small, the radiating hexagonal patch can be approximated as combination of radiating slots. For small value of width, if $a/\lambda_0 << 1$, the radiation conductance of a slot can be approximated by the following formula. [14]

$$G = \frac{1}{90}\left(\frac{a}{\lambda_0}\right)^2 \qquad (20)$$

Here, λ_0 is Free space frequency.

The current input into the side of the patch to some ports are then transmitted through the Z parameter network into the other ports and through the Radiating Edge Admittance network. If a current I_P is fed into the pth port of the antenna, which corresponds to the coaxial feed, this current is modelled with an equivalent current fed into a port on the periphery of the patch. The Z matrix parameters for the different segments shown in Figure 5 can then be written as,

$$\begin{bmatrix}\mathbf{V}_p\\ \mathbf{V}_c\\ \mathbf{V}_d\end{bmatrix} = \begin{bmatrix}\tilde{Z}_{pp} & \tilde{Z}_{pc} & \tilde{Z}_{pd}\\ \tilde{Z}_{cp} & \tilde{Z}_{cc} & \tilde{Z}_{cd}\\ \tilde{Z}_{dp} & \tilde{Z}_{dc} & \tilde{Z}_{dd}\end{bmatrix}\begin{bmatrix}\mathbf{I}_p\\ \mathbf{I}_c\\ \mathbf{I}_d\end{bmatrix} \qquad (21)$$

Here p represent the feed ports, c and d represent the interconnected ports shown in Figure 5. For a current fed in port p, the voltages at the c and d ports are given by,

$$\mathbf{V_c} = \mathbf{V_d} = [\tilde{Z}_{cp} + [\tilde{Z}_{cc} - \tilde{Z}_{cd}][\tilde{Z}_{cc} + \tilde{Z}_{dd}]^{-1}[\tilde{Z}_{dp} - \tilde{Z}_{cp}]]\mathbf{I_p} \quad (22)$$

Equation 22 can be used to calculate the voltage around the radiating edge of the patch. This voltage can be used to calculate the electric field E_Z around the periphery.

$$\mathbf{F}(\mathbf{r}) = \varepsilon_0 \int_c \frac{\mathbf{M}(\mathbf{r})}{4\pi|\mathbf{r}-\mathbf{r}'|} e^{-jk_0|\mathbf{r}-\mathbf{r}'|} dl(\mathbf{r}') \qquad (23)$$

E_Z can be represented by an equivalent magnetic current, **M**. Thus the electric vector potential at a distance **r** can be represented by Equation 23,

This equation can be written in discrete form as,

$$F(\mathbf{r}) = \varepsilon_0 \sum_1^n \frac{M_i}{4\pi|\mathbf{r}-\mathbf{r}_i'|} e^{-jk_0|\mathbf{r}-\mathbf{r}_i'|} \qquad (24)$$

As the currents in each port connected to the radiation resistances are known by applying ohms law to the voltages obtained from Equation 22, the currents M_i are obtained. The far field at distance **r** is then obtained from the components of **F**(**r**) as

$$E_\theta = \eta H_\phi = jk_0 F_\phi = jk_0(-F_x sin\phi + F_y cos\phi) \quad (25)$$

$$E_\phi = \eta H_\theta = jk_0 F_\theta = jk_0(-F_x cos\phi + F_y sin\phi)cos\theta \quad (26)$$

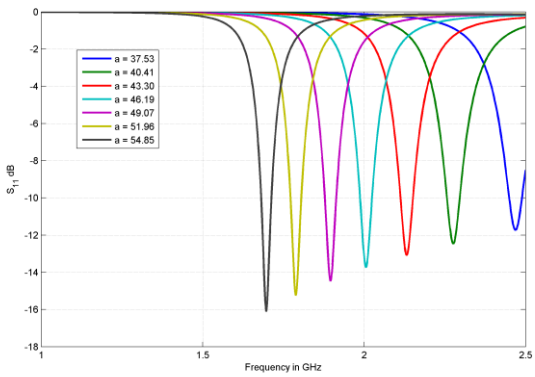

Figure 6. Return loss of basic hexagonal patch at different values of a

III. RESULTS

A. *Resonance for different patch size*

In order to find out the resonance condition of the patch, the side of the hexagon, a is varied and for different values of a, the reflection coefficient S_{11} is obtained. The result for parametric sweep is shown in Figure 6. Here, a is length of the side of a hexagon

It can be seen from Figure 6 that the resonance occurs at a particular frequency where the reflection coefficient (S_{11}) at the input port decreases rapidly. For antenna operation, the value of S_{11} in dB should be less than -10. So the frequency band between which the value stays below -10 gives an operating band.

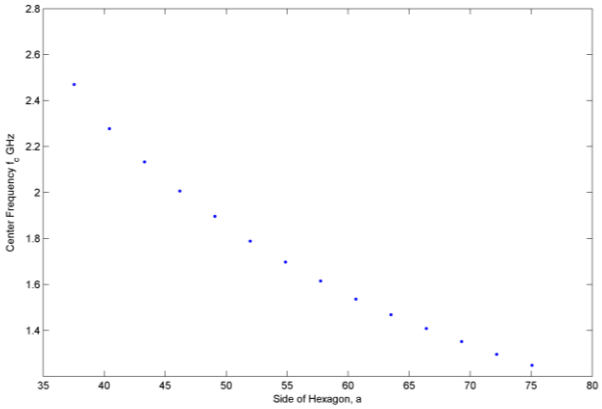

Figure 7. Center Frequency of First Band of basic hexagonal patch at different values of a

Center frequency of the first band of operation for the basic hexagonal patch decreases as the value of a increases. This is expected as the value of larger patch size implies smaller resonance frequency as the increased dimension of the patch results in larger value of capacitance as per transmission line model. The change of center frequency vs a is illustrated in Figure 7. The change of center frequency with respect to the side length can be modelled by curve fitting as,

$$f_c = -(2.1658 \times 10^{-6})x^3 + 8.2253 \times 10^{-4})x^2 - 0.11503x + 7.0548 \quad (27)$$

The simulation results are compared to an equivalent size rectangular patch antenna. The patch area in mm^2 is taken and for different patch areas the center frequency of first band and return loss bandwidth is measured. The center frequency of the rectangular patch and hexagonal patch element is shown in Figure 8. From the figure it can be seen that the center frequency of a hexagonal patch element is lower compared to the center frequency of a rectangular patch element at the same patch area. This means that for same patch area, a hexagonal patch structure can reduce the center frequency compared to a rectangular patch structure. The RL bandwidth of rectangular and hexagonal patch at different patch areas is shown in Figure 9. It can be seen that the bandwidth of hexagonal patch is comparable to the rectangular patchstructure. The percentage bandwidth for the basic hexagonal patch is around 1.8%. It can also be seen that the bandwidth is not strongly dependent on the value of a

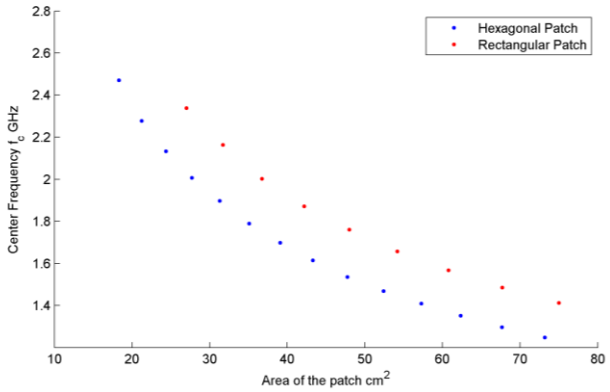

Figure 8. Center Frequency of first band vs basic hexagonal patch and rectangular patch at different values of a.

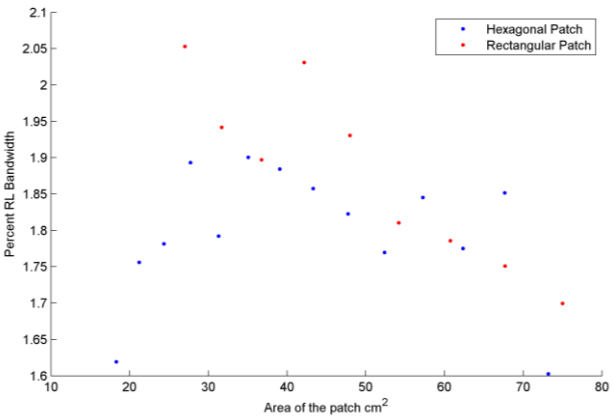

Figure 9. RL Bandwidth of first band vs basic hexagonal patch and rectangular patch at different values of a

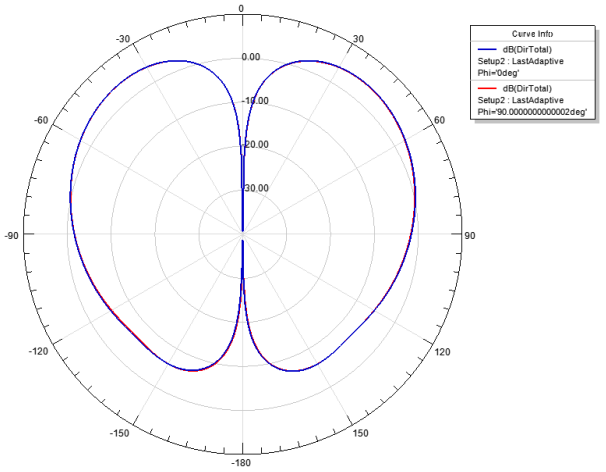

Figure 10. Radiation pattern of a hexagonal patch designed for 1.57542GHz

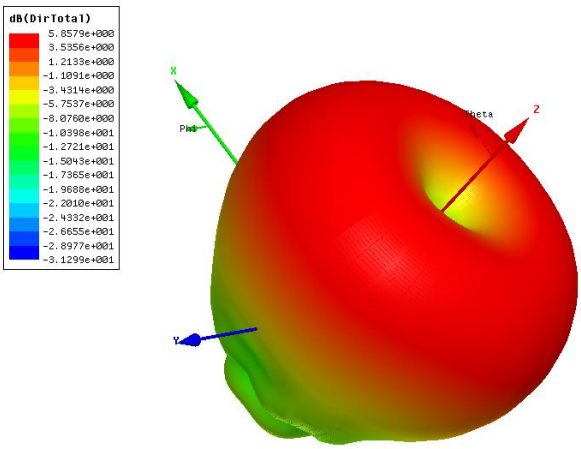

Figure 11. 3D Radiation pattern of hexagonal patch

To evaluate the far field radiation characteristics of the hexagonal patch, a patch was designed to operate at 1.57542GHz, which is the L1 frequency band of GPS. Figure 10 shows the directivity pattern for two vertical planes of the patch. Figure 11 shows 3d directivity pattern for the designed hexagonal patch

III. Conclusions

A microstrip patch antenna having a hexagonal patch structure has been studied. The multiport analysis technique is applied to the Hexagonal patch structure, and equivalent circuit model is derived. To analyze the performance of the antenna, the RL is calculated at different frequencies and the results are compared to those of rectangular patch structure. It is found that the hexagonal patch structure results in patch size reduction compared to basic hexagonal patch structure for same RL bandwidth.

References

[1] K. Carver and J. Mink, "Microstrip antenna technology," *Antennas and Propagation, IEEE Transactions on*, vol. 29, no. 1, pp. 2–24, 1981.

[2] K. C. Gupta, *Handbook of Microstrip Antennas*, ch. Multiport network approach for modelling and analysis of microstrip patch antennas and arrays, pp. 455–522. Peter Peregrinus Ltd., 1989.

[3] Y. Lo, D. Solomon, and W. Richards, "Theory and experiment on microstrip antennas," *Antennas and Propagation, IEEE Transactions on*, vol. 27, no. 2, pp. 137–145, 1979.

[4] W. Richards, Y. Lo, and D. Harrison, "An improved theory for microstrip antennas and applications," *Antennas and Propagation, IEEE Transactions on*, vol. 29, no. 1, pp. 38–46, 1981.

[5] G. Kumar and K. P. Ray, *Broadband Microstrip Antennas*. Artech House, 2003.

[6] G. Sener, "Multiport analysis by padé approximation," *Progress In Electromagnetics Research*, vol. 125, pp. 203–218, 2012.

[7] A. Farahbakhsh, S. Mohanna, and S. Tavakoli, "Reduction of return loss and mutual coupling in two-dimensional microstrip array antennas by using hexagonal patches," in *Proc. 2nd Int Mechanical and Electrical Technology (ICMET) Conf*, pp. 319–322, 2010.

[8] M. Dubey, D. Bhatnagar, V. K. Saxena, and J. S. Saini, "Broadband dual frequency hexagonal microstrip antenna for modern communication systems," in *Proc. Int. Conf. Emerging Trends in Electronic and Photonic Devices & Systems ELECTRO '09*, pp. 303–306, 2009.

[9] T. Okoshi, Y. Uehara, and T. Takeuchi, "The segmentation method–an approach to the analysis of microwave planar circuits (short papers)," *Microwave Theory and Techniques, IEEE Transactions on*, vol. 24, pp. 662 – 668, oct 1976.

[10] R. Chadha and K. C. Gupta, "Green's functions for triangular segments in planar microwave circuits," *Microwave Theory and Techniques, IEEE Transactions on*, vol. 28, no. 10, pp. 1139–1143, 1980.

[11] A. Benalla and K. C. Gupta, "Faster computation of z-matrices for rectangular segments in planar microstrip circuits (short paper)," *Microwave Theory and Techniques, IEEE Transactions on*, vol. 34, no. 6, pp. 733–736, 1986.

[12] S. H. Lee, A. Benalla, , and K. C. Gupta, "Faster computation of z-matrices for triangular segments in planar circuits," *Inrernational Journal of Microwave and Mil limeter-Wave Computer-Aided Engineering*, vol. 2, pp. 98–107, 1992.

[13] R. Garg, P. Bhartia, I. Bahl, and A. Ittipiboon, *Microstrip Antenna Design Handbook*. Artech House Inc., 2001.

[14] A. Derneryd, "Linearly polarized microstrip antennas," *Antennas and Propagation, IEEE Transactions on*, vol. 24, no. 6, pp. 846–851, 1976.